International Journal of Applied Engineering Research ISSN 0973-4562 Volume 13, Number 10 (2018) pp. 8511-8517

Hydrodynamic Force Calculation over an Axisymmetric AUV with Constant Ocean Currents at Large Range of Angles of Attack

Aguirre F.[1] [2*] Vargas S.[2] and Tornero J.[1]

[1]*Universitat Politècnica de València, Institute of Design and Manufacture, Camino de Vera S/N Edificio 8G, 46011, Valencia, España.*

[2]*Universidad Libre, Faculty of mechanical engineering, Bogotá, Colombia.*

**Corresponding author*

Abstract

Mobile robotics has allowed remote exploration of terrestrial, aerial and aquatic environments; environments that present conditions where human could not bear; e.g., extreme temperatures, extremely low or high-pressure and perform surveillance without being detected among others. The incorporation of robots in these activities reduces the risk to which a human would be exposed in these environments. In aquatic environments, specifically in ocean, there are currents that interfere in the development of missions such as data acquisition and structures overhaul, these streams affect robot activities making difficult to maintain a specific position to develop the mission accurately. The application of a control strategy that allows keeping the robot in a specific position requires of the Hydrodynamic Force generated by the marine currents. On the other hand, as the robot moves it is necessary to know the magnitude of the Hydrodynamic Force changes in the new positions.

This work was performed on a symmetric Autonomous Underwater Vehicle (AUV) Hull in the X-Y and X-Z planes in a range of attack angles from 0º to 180º. In this article, a series of simulations was developed through Computer Fluid Dynamics (CFD). This method allowed to observe three zones in the graph of the hydrodynamic coefficient (C_H) according to the angle of attack ($0^o \leq \theta \leq 25^o$, $20^o < \theta \leq 90^o$ y $90^o < \theta \leq 180^o$), for each of these zones a correlation was proposed empirical polynomial of third order to obtain the magnitude of the Hydrodynamic Force (f_H). The simulations were performed for a Reynolds number of 1.8×10^6, based on the diameter of the Hull. This methodology is proposed as a solution to evaluate in an agile and satisfactory way the Hydrodynamic Force for different orientations between the vehicle studied and the flow.

Keywords: hydrodynamics force, hydrodynamics coefficient, angle of attack, marine current, hull, autonomous underwater vehicle.

Nomenclature

f_H	=	Hydrodynamic Force
C_H	=	Hydrodynamic coefficient
ρ	=	Fluid density
R	=	Number Reynolds
Φ	=	Angle of rotation on the axis X (roll)
α	=	Angle of rotation on the axis Y (pitch)
ψ	=	Angle of rotation on the axis Z (yaw)
θ	=	Angle of attack
U	=	Flow speed
A	=	Transverse area of the AUV hull, normal to the direction of flow advance.
y^+	=	non-dimensionless distance perpendicular to the surface
u_*	=	The friction velocity at the nearest wall
τ_w	=	Shear stress at the body surface
ρ	=	Density of the fluid
ν	=	Kinematical viscosity of the fluid.

INTRODUCTION

Fluid resistance generated a hydrodynamic force (f_H) when an object moves through a fluid. This force is due to friction and pressure force and these two forces are directly proportional to the shape of the object, speed and properties of the fluid. The hydrodynamic force is opposed to the movement of the object, in an AUV this force must be overcome by the propulsion system, otherwise there would be no movement [1].

Computational fluid dynamics is a powerful tool capable to solve Navier-Stokes (N-S) equations in order to evaluate credibly the magnitude of the hydrodynamic force. In a general way, literature report that two main conditions, the vector that describes the geometry orientation and the vector of object displacement influence hydrodynamic force. Vector orientation and vector displacement are directly related to the angle of attack that describes the relation of the object's position with respect to the fluid movement [2]. To obtain reliable data results applying CFD simulations, you need a dependable CFD code and a computer system with high computational capacity in order to simulate the problem close to reality that require long time simulation due to high mesh density [3].

On the other side, mathematical modeling in mobile robotics requires the implementation of efficient calculation methods

to deliver reliable results. One of the important parameters in mobile robotics modeling applied to AUVs is the hydrodynamic force, in most of existing mathematical models of this kind the implementation of the values of the hydrodynamic force corresponds to a constant value. Taking f_H as a constant value suggests that both the vector orientation and vector of displacement of the vehicle are also constant. While in real applications of AUVs and Unmanned Aerial Vehicles (UAVs), the hydrodynamic force is certainly not constant. The f_H is affected by flow velocity and angles of attack during its trajectory. These parameters makes a mobile robotics mathematical model applied to AUVs and UAVs more complex. So mobile robotics modeling required to evaluate the magnitude of the hydrodynamic force in each instant for each angle of attack and trajectory position, this would imply a lot of time and high consumption of computational resources in the hardware and software of the robot [4] [5]. Figure 1 shows some of the important vectors on the displacement of an AUV in the development of a mission, which can changes its position with respect to a marine current. Even if the AUV is static the marine current could be changing in short periods of time.

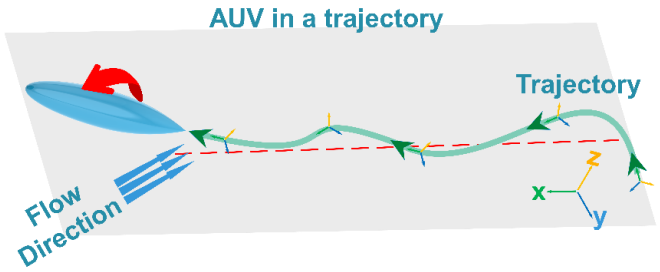

Figure 1. AUV trajectory and marine flow direction

METHODS AND MATERIALS

The AUV´s are vehicles capable to develop multiple missions. These missions can be classified into three types: (1) research missions, (2) military missions and, (3) commercial activity missions. In military missions the main objective is surveillance and persecution, these are the missions where the highest speeds are reached (7 m/s). Research missions require that AUVs to maintain their position to collect data, this implies that the AUVs are subject only to the marine current velocity which most of the time reach a speed velocity of 3 m/s, because the AUVs speed displacement is not important the advance the vehicle is slow (<1 m/s). Thus for this type of missions the velocity to calculate the hydrodynamic force is not more than 3 m/s. In commercial activity missions, high speeds are not important also. Nowadays, most of the existing AUVs are used in research activity missions, so we applied the speed conditions of these missions for this study [6].

A. Geometry of study

In this study, we analyzed an AUV hull in the form of a drop; this geometry has an excellent hydrodynamics [7]. Additionally, several authors support that five times the length to the diameter ratio of a drop shape of the hull, is the relation with the lowest hydrodynamic force [8] [9] [10]. The dimensions of the AUV hull studied here are 3 m length (L), 0.6 m diameter (D), Figure 2.

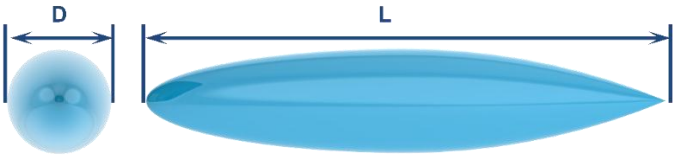

Figure 2. AUV hull geometry used for the CFD simulations

B. Problem setup

In order to guarantee that the dimensions of the control volume domain do not affect the simulations results, a minimum size must be ensured in order to obtain a fully developed flow without lateral surfaces interfere with the flow near the Hull wall. Based on the AUV hull dimensions; e. g. length (L) and diameter (D), , the size domain is 7L (21 m) upstream, 12L (36 m) downstream and 36D (21.6 m) in the Z and Y direction. Boundary and initial flow conditions: Turbulence Intensity 5%, Turbulence Viscosity Ratio 10, flow inlet velocity 3 m / s, gauge pressure outlet zero. Non-slip condition (V = 0) was applied to all lateral walls of the control volume domain. Boundary and initial conditions are illustrated in Figure 3, these dimensions allowed to pose different angles of attack by turning the hull geometry.

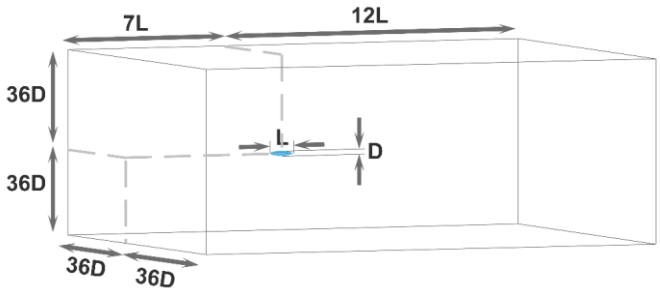

Figure 3. Boundary and initial conditions of the control volume

We did CFD simulations applying Shear Stress Transport (SST) turbulence model, this model belongs to RANS turbulence models commonly used for engineering simulations due to its robustness and application in a wide range of flows, the solver implemented in these CFD simulations series was ANSYS -Fluent V18.1 [11]. SST turbulence model is a strong combination between k-ε turbulence model and k-ω turbulence model in order to capture near-wall effects in most of the parameter close to the solid-walls, such as wall shear stress [12]. We run the simulations until residuals (continuity, velocity, kinetic energy, and turbulent frequency, drag and lift forces) convergence reached magnitudes of the order of 10^{-6}; this convergence was reached at 1 x 10^5 iterations for a second-order discretization scheme.

C. Mesh

In all the CFD simulations carried out in this work, a mixed meshing strategy was incorporated, in which techniques of unstructured mesh and structured mesh were implemented, this type of meshes is used in the analysis of irregularly shaped objects [13], the structured mesh was made near the wall of the Hull as shown in Figure 4. Additionally, for the generation of the mesh, the efforts were focused on guaranteeing the quality of the mesh close to the analysis surface using the sizing function. The inflation function was used to reduce the size of the distance perpendicular to the study surface; thus achieving a dimensionless distance (y^+) less than 2 wall units in the worst case ($\theta = 90^o$). The y^+ is a non-dimensional wall distance, which is defined in the Equation (1):

$$y^+ = \frac{u_* \times y}{v} \qquad (1)$$

Where y^+ is the distance to the body surface, u_* is the friction velocity at the nearest wall, $u_* = \sqrt{\tau_w / \rho}$, τ_w is the shear stress at the solid wall surface, ρ is the density of the fluid, y is the distance to the nearest wall and v is the local kinematic viscosity of the fluid.

All simulations were carried out within the area of the viscous sublayer ($y^+ < 5$) [13] [14] [15]. Figure 4 shows the result of the mesh and make a detailed view to observe the particularities near the wall of the hull.

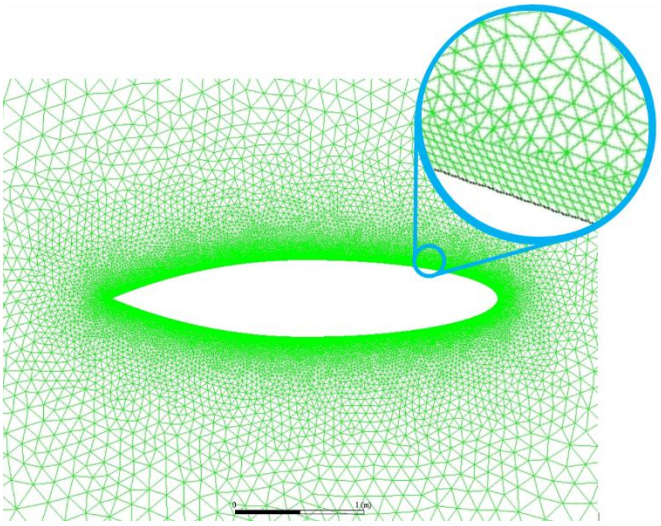

Figure 4. Grid mesh density close to the solid wall of the AUV

D. Computational simulation resources

On the simulation we used a Workstation with the following specifications, Intel Xeon processor E5-2697A v4 2.6G 16C, 18 cores, running 64 bit Windows 10 with 64 GB DDR RAM, NVidia graphics card Quadro M4000 8GB.

CASE STUDY

In this investigation a series of simulations were developed in CFD varying the angle of attack (θ) every 5º, in a range comprised between 0º and 180º, measured from the center of gravity of hull, this allowed to obtain the magnitude of the Hydrodynamic Coefficient (C_H). Figure 5 shows the conditions in which variations of the angle of attack were proposed. For our study the angle of attack (θ) coincides with the pitch angle (α).

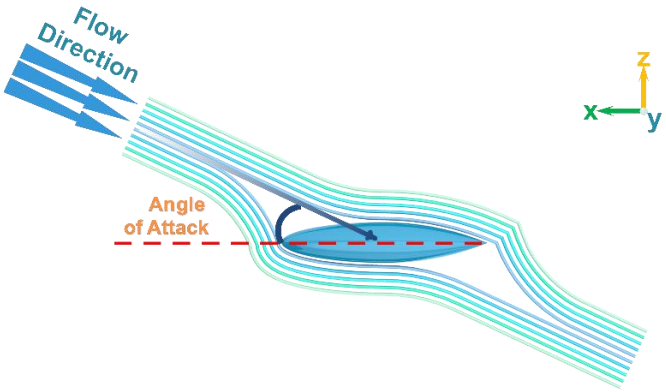

Figure 5. Angle of attack

In nature, an object moving in the interior of a fluid the hydrodynamic force cannot be neglected. Thus quantifying the magnitude of the hydrodynamic force makes possible to estimate with precision the power required to reach the desired displacement speed or the stability of the object under study [17]. The hydrodynamic force can also allow us to estimate with precision the energy consumption required to perform a mission [18]. On the other hand, CFD simulation can be useful to improve parameters to optimize the shape of a design [19].

The hydrodynamic force has three components, drag force aligned with the flow direction, (2) lift force perpendicular to the flow direction (upwards or downwards) and (3) side force transversal to the flow direction (left or right), in Figure 6 these components are shown on the object of analysis.

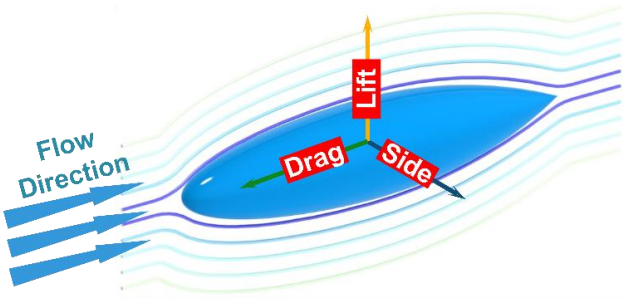

Figure 6. Components of the hydrodynamic force

In general, the calculation of the hydrodynamic force of an object immersed in a fluid can be calculate by Equation (2)

$$f_H = \frac{1}{2}\rho A_c v^2 c_H \qquad (2)$$

In the displacement or stability of an AUV flow currents can arrive with any angle of attack. In a three-dimensional problem, that is the case of an AUV, the possibility of the angle of attack changing increases. In this study, the angle of attack is measured between the longitudinal axis of the AUV and the fluid flow main direction vector. The cases analyzed in this investigation consider several orientations given by an angle of rotation, Φ = angle of rotation on the axis X (angle roll), α = angle of rotation on the axis Y (pith angle) and ψ = angle of rotation on the axis Z (yaw angle).

The marine currents are generated mainly by three factors, (1) the earth movement rotation and translation, (2) winds and (3) the temperature difference between the deep and superficial waters. Advanced research tidal energy transformation has quantified the speed of marine currents by averaging them at six nodes (~ 3 m / s) [20]. As mentioned before, a large percentage of AUVs are used in research missions, for this reason the development conditions of these missions are specifically addressed in this work, the need to maintain a position to take data. Thus, the hydrodynamic force will be estimated on the AUV assuming a velocity speed of 3 m / s.

We development CFD simulations varying the angle of attack as shown in Figure 7; estimating the orientation of the vector in three dimensions.

In order to calculate the magnitude of the hydrodynamic force for every angle of attack, it is necessary to evaluate the C_H and apply Equation 2. In this study we assumed constant cross-sectional area (A_c), velocity (v) and we also considered that fluid conditions do not change, e. g., constant density (ρ). Under these conditions, we evaluated the hydrodynamic coefficient as a function of the angle of attack (θ).

For our simulations in this study, we assumed that the AUV is in a research mission and requires maintaining a position for data collection. The AUV is always in water that maintains its constant density. For all angles of attack variations the cross sectional area was constant and we assumed a constant velocity of marine current of 3 m/s. Under these conditions, we expressed the equation for hydrodynamic force as (Equation 3):

$$f_H = cte\ C_H \qquad (3)$$

The magnitude of C_H is obtained through CFD simulations as a function of angle of attack. Using the polynomial regression method, we obtained a third-order polynomial correlation to predict the values of the Hydrodynamic Coefficient for any angle of attack. Thus, with this empirical correlation it is possible directly calculate the hydrodynamic force for any angle of attack at which the AUV is subjected.

RESULTS

This section describe the CFD simulations, Figure 8 qualitatively describe the velocities field applying streamlines as a function of the angle of attack (θ). The flow direction is from left to the right for θ = 0º and change as the angle of attack increases. For θ = 180º the flow direction is from right to the left. Velocity streamlines for all angles of attack clearly shows the AUV hydrodynamics. For θ = 0º and θ = 180º streamlines show an excellent streamlined AUV hull, while for intermediate angles of attack (15º ≤ θ ≤ 165º) the velocity streamlines are disturbed generating some turbulence in the back of the flow. This phenomena is quite evidently for θ = 90º.

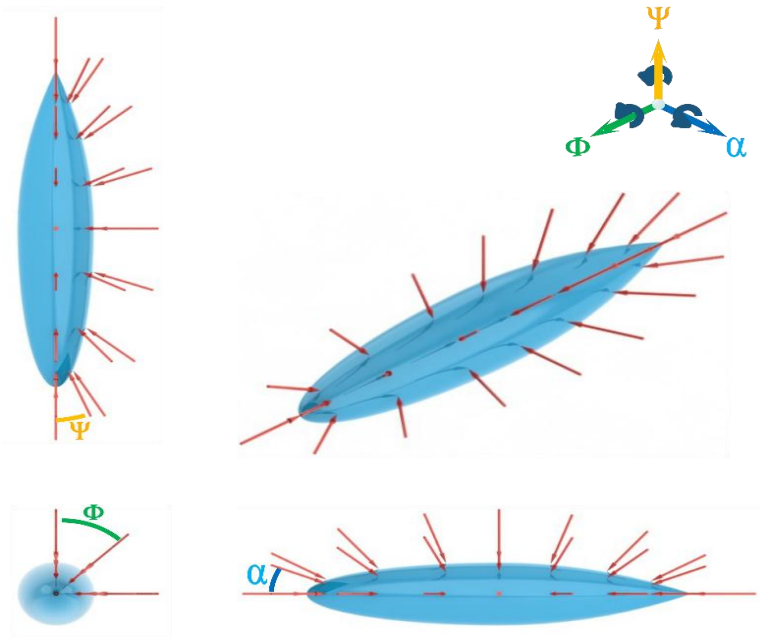

Figure 7. Vector of flow

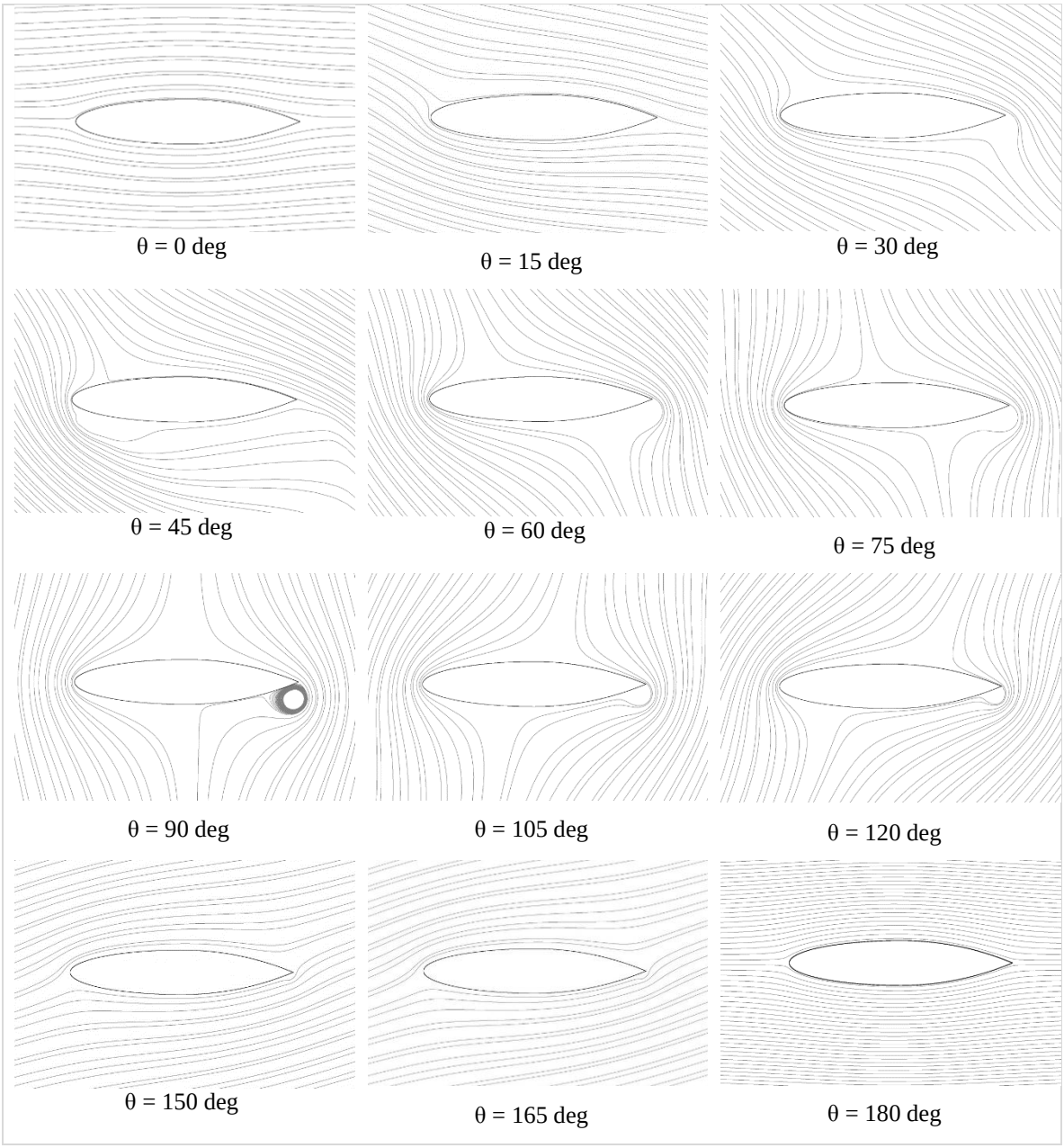

Figure 8. Speed current lines

The AUV hull is symmetrical in the X-Y and X-Z planes, therefore the hydrodynamic force for any yaw and pitch angle the magnitude of the hydrodynamic force on these two axes could be consider negligible. However, when the angle of attack (θ) is 90º, the hydrodynamic force have the greatest magnitude since the transversal area at this angle is the greatest and consequently pressure forces are predominant under these conditions. On the other hand, angles of attack of θ = 0º and θ = 180º produced minimum values of hydrodynamic force. For these two angles of attack, the longitudinal axis (X) of the hull is parallel to the flow direction and due to the shape of the AUV hull transversal area is the small and both pressure and friction forces are relatively small because of the excellent hydrodynamics of the AUV geometry.

Simulated C_H coefficients and its variation with angle of attack in the range of θ = 0º to θ = 90º for a Reynolds number of 1.8 x 10^6 are presented in Figure 9. We found three main patterns of C_H, the first one from θ = 0º to θ = 25º, the second one from θ > 25º to θ = 90º and the third one from θ > 90º to θ = 180º. Very small values of C_H are observed at θ = 0º and θ = 180º, these values are of the order of 9 x 10^{-3}. The greatest value of C_H = 2.9 found at θ = 90º as shown in the graph of Figure 9.

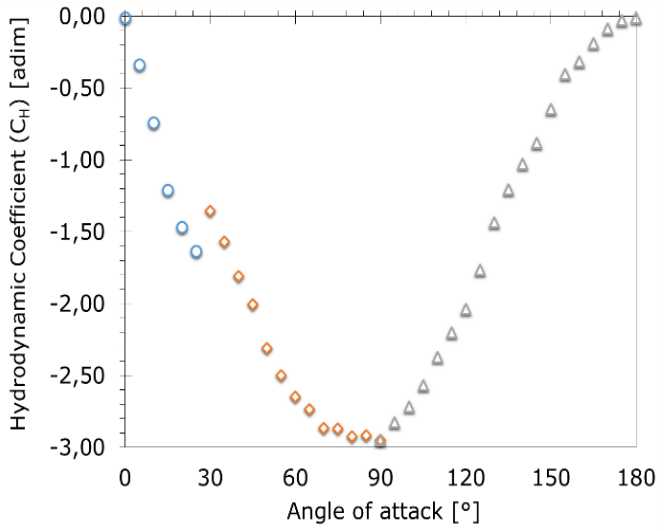

Figure 9. CFD simulations Hydrodynamic Coefficient vs. Angle attack

Due to the discontinuities found in the C_H graph of the Figure 9, we decided to divide the total C_H data results into three different sections. The first one ($0^o \leq \theta \leq 25^o$) is shown in Figure 10, the second one in the range of $\theta > 25^o$ and $\theta \leq 90^o$ shown in Figure 11 and third one between $90^o \leq \theta \leq 180^o$ shown in Figure 12.

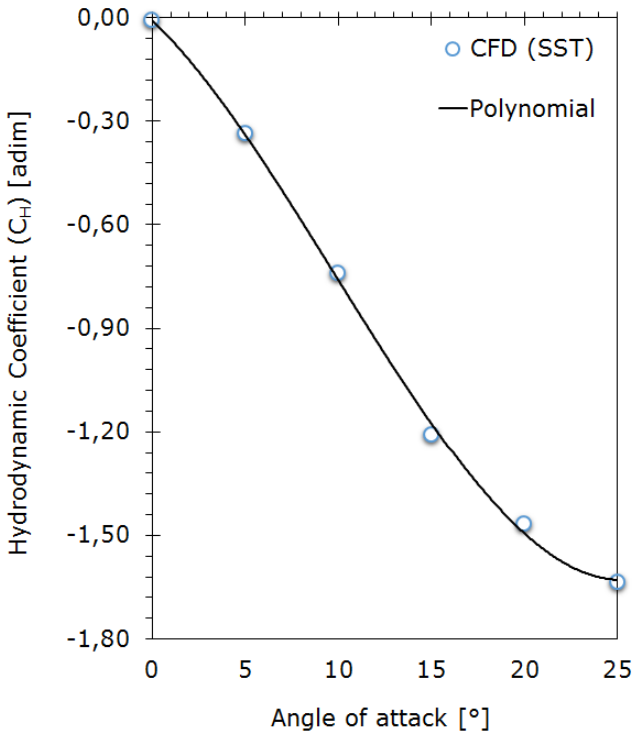

Figure 10. Hydrodynamic Coefficient $0^o < \theta < 25^o$

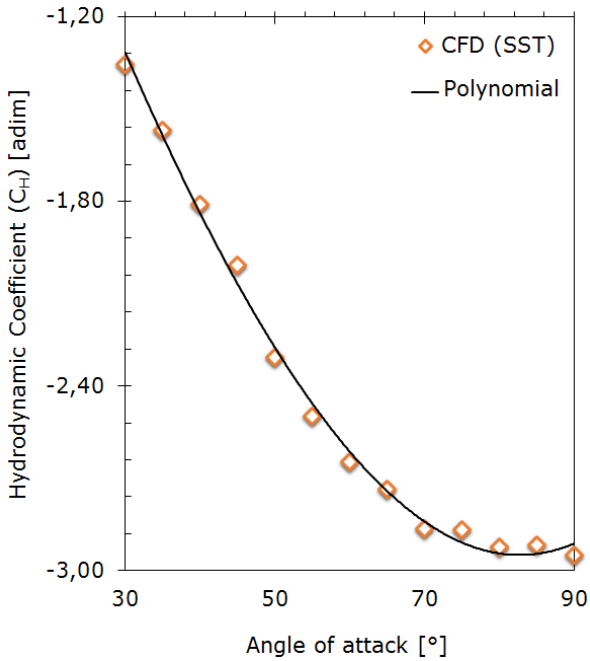

Figure 11. Hydrodynamic Coefficient $25^o < \theta < 90^o$

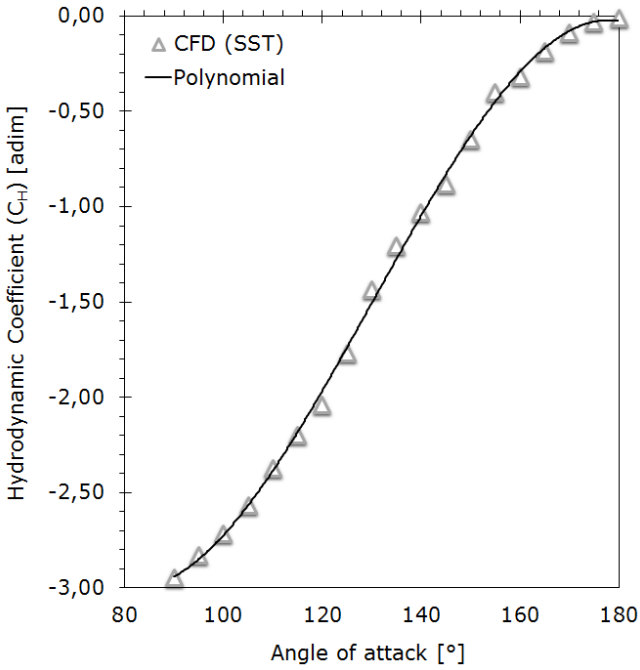

Figure 12. Hydrodynamic Coefficient $90^o < \theta < 180^o$

We proposed a third order polynomial equation for each section, according to the three section of C_H data results. The determination coefficient (R^2) for all cases was greater than 99.6%, which means an excellent agreement between the empirical correlations and the CFD simulations data results, Equation 4.

$$C_H = A\theta^3 + B\theta^2 + C\theta + D \quad \text{Equation (4)}$$

Where θ is the angle of attack in degrees, A, B, C and D are constants and their values depend on the section, see Table 1.

Table 1. Values of the constants for each section in Equation 4

Section	A (10^{-4})	B (10^{-4})	C (10^{-4})	D (10^{-4})
1 ($0^o \leq \theta \leq 25^o$)	1	-36	-514	-66
2 ($25^o < \theta \leq 90^o$)	0.02	2	-719	6280
3 ($90^o < \theta \leq 180^o$)	-0.07	26	-2953	72429

CONCLUSIONS

The major conclusions of this study are as follows:

After a series of CFD simulations, we quantify the hydrodynamic force exerted on an AUV hull by varying the angle of attack of the marine current at 3 m/s with a Reynolds number of 1.8 $x10^6$. Angle of attack directly influences that the transverse area modifying the magnitude of the pressure hydrodynamic force for $\theta = 90^o$, where the total hydrodynamic force is more than 300 times compared with the hydrodynamic force at $\theta = 0^o$ and $\theta = 180^o$.

We identified three sections in the C_H graph and proposed a polynomial equation of third order for each section with an excellent agreement between empirical equations and CFD data simulations obtained with SST-RANS turbulence model with a second order discretization scheme.

The methodology applied in this research contribute to the approach of control methods of mobile robotics (AUVs) to guarantee the stability and precision of the AUV movement in research missions where data collection is required. Data collection performed at lower velocities than 3 m/s is essential, e.g., inspection, filming and scanning activities.

The obtained fitted polynomials are useful to evaluate f_H with an error of less than 3%, thus the fitted curves show a reliable application in dynamic and kinematic modeling of AUV.

REFERENCES

[1] Hoerner, S. F. (1965). Fluid-dynamic drag: practical information on aerodynamic drag and hydrodynamic resistance (p. 598). Midland Park, NJ: Hoerner Fluid Dynamics.

[2] Johnson, R. W. (Ed.). (2016). Handbook of fluid dynamics. Crc Press.

[3] de Barros, E. A., Dantas, J. L., Pascoal, A. M., & de Sá, E. (2008). Investigation of normal force and moment coefficients for an AUV at nonlinear angle of attack and sideslip range. IEEE Journal of Oceanic Engineering, 33(4), 538-549.

[4] Chen, C. W., Kouh, J. S., & Tsai, J. F. (2013). Modeling and simulation of an AUV simulator with guidance system. IEEE Journal of Oceanic Engineering, 38(2), 211-225.

[5] Valavanis, K. P., & Vachtsevanos, G. J. (2014). Handbook of unmanned aerial vehicles. Springer Publishing Company, Incorporated.

[6] Aguirre F.; Vargas S.; Valdés D. and J. Tornero (2017) International Journal of Oceans and Oceanography, ISSN 0973-2667 Volume 11, Number 1, pp. 89-103

[7] Zhang, H. X., & Pan, Y. C. (2006). Application CFD to compare submarine hull forms. Journal of Ship Mechanics, 10(4), 1.

[8] Miller, T. F., Gandhi, F. S., & Rufino, R. J. (2014). Morphing hull concept for underwater vehicles. Ocean Engineering, 92, 92-102.

[9] Aguirre, F., Grau, F., & Tornero, J. (2011). Optimal design parameters of AUV hull based on CFD simulation. Instrumentation viewpoint, (11), p18.

[10] Stevenson, P., Furlong, M., & Dormer, D. (2007, June). AUV shapes-combining the practical and hydrodynamic considerations. In Oceans 2007-Europe (pp. 1-6). IEEE.

[11] Xuliang, Y., Lingwei, M., Feng, W., & Xiaoli, N. (2016, April). Investigation of thrust and load characteristics of AUV propeller under the condition of different angle incoming flow. In OCEANS 2016-Shanghai (pp. 1-5). IEEE.

[12] Yun, alexander, (2017). Computational fluid dynamics: from zero to guru, First edition, CreateSpace Independent Publishing Platform, Los Angeles, USA.

[13] Yuan, Y. O., Zurek, B., Liu, F., deMartin, B., & Lacasse, M. D. (2017, December). Numerical comparisons of ground motion predictions with kinematic rupture modeling. In AGU Fall Meeting Abstracts.

[14] Tu, J., Yeoh, G. H., & Liu, C. (2018). Computational fluid dynamics: a practical approach. Butterworth-Heinemann.

[15] Zangeneh, R., & Ollivier-Gooch, C. F. (2017). Mesh optimization to improve the stability of finite-volume methods on unstructured meshes. Computers & Fluids, 156, 590-601.

[16] ANSYS. (2018). Fluent 18.1 user's guide. ANSYS FLUENT Inc.

[17] Ahsan, S. N., & Aureli, M. (2017). Three-dimensional analysis of hydrodynamic forces and power dissipation in shape-morphing cantilevers oscillating in viscous fluids. International Journal of Mechanical Sciences.

[18] d'Amore-Domenech, R., Raso, M. A., Villalba-Herreros, A., Santiago, Ó., Navarro, E., & Leo, T. J. (2018). Autonomous underwater vehicles powered by fuel cells: Design guidelines. Ocean Engineering, 153, 387-398.

[19] Hang Hou, Y., Liang, X., & yang Mu, X. (2018). AUV hull lines optimization with uncertainty parameters based on six sigma reliability design. International Journal of Naval Architecture and Ocean Engineering.

[20] Ponta, F. L., & Jacovkis, P. M. (2008). Marine-current power generation by diffuser-augmented floating hydro-turbines. *Renewable energy*, *33*(4), 665-673.